NASA TECHNICAL MEMORANDUM NASA TM 75719

DETERMINATION OF THE TECHNICAL CONSTANTS OF LAMINATES IN OBLIQUE DIRECTIONS

F. Vidouse

Translation of "Determination des constantes techniques des stratifies dans les directions obliques - Theorie et resultats experimentaux", Centre de Recherches Scientifiques et Techniques de l'Industrie des Fabrications Metalliques: Brussels, Belgium, Report, CRIF PL-4, November 1973, pp 1-42

(NASA-TM-75719) DETERMINATION OF THE TECHNICAL CONSTANTS OF LAMINATES IN OBLIQUE DIRECTIONS (National Aeronautics and Space Administration) 43 p HC A03/MF A01 CSCL 11D N80-19207

G3/24 Unclas 47454

NATIONAL AERONAUTICS AND SPACE ADMINISTRATION
WASHINGTON, D.C. 20546 OCTOBER 1979

STANDARD TITLE PAGE

1. Report No. NASA TM 75719	2. Government Accession No.	3. Recipient's Catalog No.
4. Title and Subtitle DETERMINATION OF THE TECHNICAL CONSTANTS OF LAMINATES IN OBLIQUE DIRECTIONS		5. Report Date OCTOBER 1979
		6. Performing Organization Code
7. Author(s) FERNAND VIDOUSE, Centre de Recherches Scientifiques et Techniques de l'Industrie des Fabrications Metalliques (Brussels, Belgium)		8. Performing Organization Report No.
		10. Work Unit No.
9. Performing Organization Name and Address LEO KANNER ASSOCIATES Redwood City, California 94063		11. Contract or Grant No. NASw- 3199
		13. Type of Report and Period Covered TRANSLATION
12. Sponsoring Agency Name and Address NATIONAL AERONAUTICS AND SPACE ADMINISTRATION, Washington, DC 20546		14. Sponsoring Agency Code

15. Supplementary Notes Translation of "Determination des constantes techniques des stratifies dans les directions obliques - Theorie et resultats experimentaux", Centre de Recherches Scientifiques et Techniques de l'Industrie des Fabrications Metalliques, Brussels, Belgium, Report, CRIF PL-4, November 1973, pp 1-42 (N74-21166)

16. Abstract "An off-axis tensile test theory based on Hooke's Law and applied to glass fiber-reinforced laminates is presented. It aims at taking into account the anisotropy of the laminates. The theory introduces a corrective parameter dependent on the characteristics of the strain gauge used in order to account for the parasitic moments introduced when using common testing machines set up for isotropic materials. Theoretical results were compared for a variety of strain gauges with those obtained by a finite element method and with experimental results obtained on laminates reinforced with glass in various ways."

17. Key Words (Selected by Author(s))	18. Distribution Statement UNCLASSIFIED - UNLIMITED

19. Security Classif. (of this report) UNCLASSIFIED	20. Security Classif. (of this page) UNCLASSIFIED	21. No. of Pages 43	22. Price

NASA-HQ

TABLE OF CONTENTS

SYMBOLS

$2b$	:	width of the test piece
$2c$	:	extensometer measurement base
$2d$	:	length of the transverse gauge (see Figure 5)
e	:	thickness of the test piece
E	:	modulus of elasticity
G	:	modulus of slippage
ℓ	:	length of the test piece
m	:	surface glass content
P	:	load applied to the test piece
S_{ij}	:	matrix of flexibility
T	:	glass content by weight
T_1	:	coefficient defined in Section 4.1
u, v	:	displacement along the x and y axes
x, y	:	axial orientation of the test piece
$1, 2$	:	orientation of the principal axes of the test piece
α	:	term defined in equation (30)
β	:	term defined in equation (30)
γ	:	angular deformation
ε	:	normal deformation
$(1 - \zeta)$	:	correction coefficient for the Poisson coefficient (compare equations (37) and (38))
η_{xy}, η_{yx}	:	coupling coefficients
$(1 - \eta_I)$ $(1 - \eta_{II})$	:	correction coefficients for the modulus of elasticity
θ	:	angle formed by the fibers and the x-axis of the test pieces
ν	:	Poisson coefficient
ξ	:	term defined in equation (30)
σ	:	normal strain
τ	:	tangential strain
ϕ	:	glass content by volume
$(1 - \psi)$	:	correction coefficient for the Poisson coefficient (compare equations (37) and (38))
Ω	:	section of the test piece

INDICES

m	:	matrix
f	:	fibers
*	:	indicates an apparent magnitude yielded by the measurements

DETERMINATION OF THE TECHNICAL CONSTANTS OF LAMINATES IN OBLIQUE DIRECTIONS

F. Vidouse
Metallic Manufacturing Industry Scientific and
Technical Research Center

Summary

An off-axis tensile test theory is explained and coefficients are given to correct experimental results obtained working on usual testing machines. Theoretical results are compared with those obtained by R.M. Courtade with a finite element method and with experimental results obtained on laminates reinforced with glass in various ways.

Introduction /1*

This work constitutes the fourth part of the research undertaken by the Centre de Recherches Scientifiques et Techniques de l'Industrie des Fabrications Metalliques [Metallic Manufacturing Industry Scientific and Technical Research Center] (CRIF) on dimensioning of reinforced plastics, at the request of the industrial members of the Fabriplast Group of Fabrimetal.

Previously published papers concerning this research are the following:

— "Relation entre l'etat de polymerisation, la fatigue et le fluage d'une resine epoxy renforcee au verre textile" [Relation between the State of Polymerization, Fatigue and Flow of a Fiberglass-Reinforced Epoxy Resin] (CRIF Publication PL 1)

— "Study for polymerization and curing of polyester and epoxy resins by the dilatometric and resistivimetric methods" (CRIF Publication PL 2)

— "Theoretical and experimental study of the technical constants of laminates" (CRIF Publication PL 3)

*Numbers in the margin indicate pagination in the foreign text.

This study, like the preceding ones, is the result of collaboration between various research organizations:

— the Centre Europeen de Recherches et Essais [European Research and Testing Center] (CERE) of the Fiberglass Division of Saint-Gobain Industries at Chambery manufactured the rest materials and participated in interpretation of the results;

— the Institut National des Sciences Appliquees [National Applied Sciences Institute] (INSA) of Lyon performed the calculations according to the finite element theory;

— the Laboratoire de Resistance des Materiaux [Materials Resistance Laboratory] of the University of Liege performed the tests and contributed to analysis of the results; and lastly,

— the CRIF, acting as scientific coordinator, exploited the results and assumed scientific and technical resplosibility for the work.

The CRIF is very grateful to these various organizations, without whose assistance the research could not have been successfully concluded.

1. Purpose of Tests /2

At the time when work was being done as reported in the paper entitled "Theoretical and experimental study of the technical constants of laminates" [1], traction tests in directions other than principal directions were carried out on the same laminates. Since these tests were carried out in a conventional manner, the results cannot be directly exploited but must be corrected in order to take into account the coupling phenomenon between traction and shear.

The purpose of this work is to analyze technical constants in oblique directions and to demonstrate that it is possible to predetermine them theoretically with adequate precision.

Correction coefficients have been determined, based on an approximate elastic theory, and verified for one type of laminate with an exact theory utilizing finite elements. (It will be recalled that this method consists of cutting the structure under study into a finite number of areas with simple geometric shapes termed "finite elements" (in this case, rectangles) and subsequently rejoining these areas with the aid of a computer.) These coefficients take into account particularly the type of extensometer utilized and the geometric parameters of the test.

2. Approximate Theory of Traction Tests in Oblique Directions /3

2.1 General

As demonstrated by the generalization of Hooke's Law [1], a simple traction test on an anisotropic material induces not only normal deformation ε, but also tangential deformations γ.

Reportedly there is coupling of traction and shear effects.

$$\begin{bmatrix} \varepsilon_x \\ \varepsilon_y \\ \gamma_{xy} \end{bmatrix} = \begin{bmatrix} S_{11} & S_{12} & S_{16} \\ S_{12} & S_{22} & S_{26} \\ S_{16} & S_{26} & S_{66} \end{bmatrix} \begin{bmatrix} \sigma_x \\ 0 \\ 0 \end{bmatrix} \qquad (1)$$

This equation demonstrates that ε_y and γ_{xy} are not non-existent when S_{16} and S_{26} are not zero.

Experience also demonstrates clearly that warping occurs during a traction test to the extent allowed by the anchorage of the ends of the test piece (Figure 1).

Figure 1 illustrates the deformation of a test piece made of a material which is not symmetric with respect to thickness. If the material is symmetric, warping occurs only on the plane surface of the test piece (Figure 4).

Conventional test equipment, designed for isotropic materials, does not allow the ends of the test pieces to be rotated. When traction tests of anisotropic materials are carried out using this equipment, parasitic moments are introduced which could invalidate the results. The following theory is intended to calculate the error introduced by this procedure, and to correct the values obtained, by means of a coefficient which, as will be shown, depends particularly on the type of extensometer utilized.

Various types of extensometers exist, differing particularly with respect to the test piece attachment means. As shown in Figure 2, the relative position of the feelers can vary: the Type I extensometer has feelers placed on both sides of the test piece while the Type II extensometer has feelers only on one side. The Type I and Type II extensometers are located at the edge of the test piece. The Type III extensometer is similar to the Type II extensometer, but its feelers rest on one of the surfaces of the test piece. Lastly, the Type IV extensometer is an axially oriented strain gauge.

2.2 Traction Test Theory /4

2.2.1 Compatibility Equation

The analytic solution of the problem is obtained by applying the theory of elasticity [2].

The reference axis orientation is illustrated in Figure 3.

The following relations must be satisfied [4]:

— equilibrium equations:

$$\frac{\partial \sigma_x}{\partial x} + \frac{\partial \tau_{xy}}{\partial y} = 0$$

$$\frac{\partial \sigma_y}{\partial y} + \frac{\partial \tau_{xy}}{\partial x} = 0 \qquad (2)$$

— deformation/displacement relations:

$$\begin{aligned} \varepsilon_x &= \frac{\partial u}{\partial x} \\ \varepsilon_y &= \frac{\partial v}{\partial y} \\ \gamma_{xy} &= \frac{\partial u}{\partial y} + \frac{\partial v}{\partial x} \end{aligned} \tag{3}$$

— the generalization of Hooke's Law:

$$\begin{bmatrix} \varepsilon_x \\ \varepsilon_y \\ \gamma_{xy} \end{bmatrix} = \begin{bmatrix} S_{11} & S_{12} & S_{16} \\ S_{12} & S_{22} & S_{26} \\ S_{16} & S_{26} & S_{66} \end{bmatrix} \begin{bmatrix} \sigma_x \\ \sigma_y \\ \tau_{xy} \end{bmatrix} \tag{4}$$

When the displacement terms in equations (3) are removed, deformations as a function of strain with relations (4) are subsequently expressed, and equations (2) are utilized to find the compatibility equation:

$$\begin{aligned} &(2S_{12} + S_{66}) \frac{\partial^2 \sigma_x}{\partial x^2} + S_{11} \frac{\partial^2 \sigma_x}{\partial y^2} - 2 S_{16} \frac{\partial^2 \sigma_x}{\partial x \partial y} \\ &- 2S_{26} \frac{\partial^2 \sigma_y}{\partial x \partial y} + S_{22} \frac{\partial^2 \sigma_y}{\partial x^2} = 0 \end{aligned} \tag{5}$$

The S_{ij} matrix is termed the matrix of flexibility. /5

Utilizing the notation selected by Ashton and Whitney [4], flexibilities are expressed as functions of technical constants according to the following relations:

$$S_{11} = \frac{1}{E_{xx}} \qquad S_{22} = \frac{1}{E_{yy}} \qquad S_{66} = \frac{1}{G_{xy}}$$

$$S_{12} = -\frac{\nu_{xy}}{E_{xx}} = -\frac{\nu_{yx}}{E_{yy}}$$

$$S_{16} = -\frac{\eta_{xy}}{E_{xx}} \tag{6}$$

$$S_{26} = -\frac{\eta_{yx}}{E_{yy}}$$

2.2.2 Limit Conditions

If one end of the test piece ($x = 0$) is held by rigid clamps, the limit conditions can be written in the following way:

$$v\ (0,y) = 0 \qquad \frac{\partial u\ (0,y)}{\partial y} = 0 \tag{7}$$

Since the edges of the test piece are free, it follows:

$$\sigma_y\ (x,\pm b) = \tau_{xy}\ (x,\pm b) = 0 \tag{8}$$

The analytic solution satisfying these conditions is extremely complex, or even impossible.

Equations (7) can be replaced by the following limit conditions which are partially justified by experience:

$$\begin{aligned} &v\ (0,0) = 0 \qquad \frac{\partial u\ (0,0)}{\partial y} = 0 \qquad u\ (0,0) = 0 \\ &v\ (\ell,0) = 0 \qquad \frac{\partial u\ (\ell,0)}{\partial y} = 0 \qquad u\ (\ell,0) = \varepsilon_0 \ell \end{aligned} \tag{9}$$

where ε_0 is a deformation proportional to the magnitude of the applied force P.

2.2.3 Strain and Displacement Expressions

Since shear is independent of x, it can be posited:

$$\tau_{xy} = f\,(y) \tag{10}$$

By integration in (2), it follows: /6

$$\begin{aligned} \sigma_x &= -\,x\,f'\,(y) + g\,(y) \\ \sigma_y &= h\,(x) \end{aligned} \tag{11}$$

Taking into account the condition for compatibility (5) and preceding relations, we obtain:

$$\begin{aligned} f\,(y) &= C_0\,(y^2 - b^2) \\ g\,(y) &= -\,2\,\frac{S_{16}}{S_{11}}\,C_0 y^2 + C_1 y + C_2 \\ h\,(x) &= 0 \end{aligned} \tag{12}$$

where C_0, C_1 and C_2 are integration constants.

From (4), (11) and (12), the strain and deformation expressions can be obtained quite easily:

$$\begin{aligned} \sigma_x &= -\,2C_0 xy - 2\,\frac{S_{16}}{S_{11}}\,C_0 y^2 + C_1 y + C_2 \\ \sigma_y &= 0 \\ \tau_{xy} &= C_0\,(y^2 - b^2) \end{aligned} \tag{13}$$

$$\begin{aligned} \varepsilon_x &= S_{11}\,(-2C_0 xy + C_1 y + C_2) - S_{16} C_0\,(y^2 + b^2) \\ \varepsilon_y &= S_{12}\,(-2C_0 xy - 2\,\frac{S_{16}}{S_{11}}\,C_0 y^2 + C_1 y + C_2) + S_{26} C_0\,(y^2 - b^2) \\ \gamma_{xy} &= S_{16}\,(-2C_0 xy - 2\,\frac{S_{16}}{S_{11}}\,C_0 y^2 + C_1 y + C_2) + S_{66} C_0\,(y^2 - b^2) \end{aligned} \tag{14}$$

By integration, the following displacement expressions are found:

$$
\begin{aligned}
u = & - S_{16}C_0x\,(y^2 + b^2) + S_{11}x\,(C_2 + C_1y - C_0xy) + C_5 \\
& + (S_{16}C_2 - S_{66}C_0b^2 - C_3)y + \frac{S_{16}C_1y^2}{2} \\
& + \frac{C_0y^3}{3}\left(S_{12} + S_{66} - \frac{2S_{16}^2}{S_{11}}\right) \\
v = & \ S_{12}y\left(-\frac{2}{3}\frac{S_{16}}{S_{11}}C_0y^2 + \frac{C_1y}{2} + C_2 - C_0xy\right) \\
& + \frac{S_{26}C_0y}{3}(y^2 - 3b^2) + C_4 + C_3x - \frac{S_{11}C_1x^2}{2} + \frac{S_{11}C_0x^3}{3}
\end{aligned}
\qquad (15)
$$

The integration constants are obtained by expressing the limit conditions: /7

$$
\begin{aligned}
C_0 &= \frac{6\,S_{16}\,\varepsilon_0}{6b^2(S_{11}S_{66} - S_{16}^2) + S_{11}^2\ell^2} & C_3 &= \frac{C_0S_{11}\ell^2}{6} \\
C_1 &= C_0\ell & C_4 &= 0 \\
C_2 &= \frac{C_0}{6\,S_{16}}(6\,S_{66}b^2 + S_{11}\ell^2) & C_5 &= 0
\end{aligned}
\qquad (16)
$$

2.2.4 Magnitudes Yielded by the Test

The traction test allows determination of two technical constants: the modulus of elasticity and the Poisson coefficient of the material, while simultaneously recording the (ε_x, P) and (ε_y, ε_x) or (ε_y, P) graphs.

These measurements can be made without any particular difficulty for isotropic materials, regardless of the type of extensometer utilized.

In the case of anisotropic materials, the field of deformation is not uniform, as shown in Figure 4, as charted for a flexible material utilizing equations (15) (E_{11} = 8 kg/mm^2, E_{22} = 0.5 kg/mm^2, ν_{12} = 0.5, ν_{21} = 0.03125, G_{12} = 0.2 kg/mm^2) for elongation of ε_0 = 20 percent.

Therefore, for these materials, it is necessary to examine more closely the magnitudes actually yielded by the measurement equipment. In the case of Figure 5, the test piece is fitted with a Type I extensometer (see Figure 2a) whose feelers are located at points A and B and with a transverse strain gauge whose ends are located at points C and D.

Proceeding in the same manner as for isotropic materials, the magnitudes measured are the following:

$$E^{\star}_{xx} = \frac{\sigma^{\star}_x}{\varepsilon^{\star}_x} \qquad \nu^{\star}_{xy} = \frac{\varepsilon^{\star}_y}{\varepsilon^{\star}_x} \tag{17}$$

with

$$\sigma^{\star}_x = \frac{P}{\Omega} = \frac{P}{2eb}$$

In fact, the values obtained (denoted by asterisks) are not exact.

The extensometer does not yield ε_x but (see Figure 5) does yield: /8

$$\varepsilon^{\star}_x = \frac{u_B - u_A}{2c} \tag{18}$$

Likewise, the transverse strain gauge yields:

$$\varepsilon^{\star}_y = \frac{v_D - v_C}{2d} \tag{19}$$

The expression of $\sigma^{\star}_x$ is written:

$$\sigma^{\star}_x = \frac{P}{2be} = \frac{1}{2b} \int_{-b}^{b} \sigma_x \, dy \tag{20}$$

Therefore, the measured constants $E^{\star}_{xx}$ and $\nu^{\star}_{xy}$ must be modified by correction coefficients, to be determined, such as:

$$E_{xx} = \frac{1}{S_{11}} = E^{\star}_{xx} (1 - \eta) \tag{21}$$

$$\nu_{xy} = - E_{xx} S_{12} = \nu^{\star}_{xy} (1 - \zeta) \tag{22}$$

2.2.5 Correction Coefficients for the Modulus of Elasticity

Let us consider the Type I extensometer as shown in Figure 5. When σ_x is replaced in equation (20) by its expression (13), and relations (16) are taken into account, the expression of σ_x^* is written:

$$\sigma_x^* = C_0 \left[b^2 \left(\frac{S_{66}}{S_{16}} - \frac{2}{3} \frac{S_{16}}{S_{11}} \right) + \frac{\ell^2}{6} \frac{S_{11}}{S_{16}} \right] \tag{23}$$

The coordinates of extensometer feeler application points A and B are, respectively:

$$A \left(\frac{\ell}{2} - c \; ; \; b\right) \quad \text{et} \quad B \left(\frac{\ell}{2} + c \; ; \; - b\right) \qquad [23a]$$

When u_A and u_B are calculated by means of relation (15) and are replaced in equation (18), we obtain:

$$\varepsilon_x^* = C_0 S_{11} \left[- \frac{1}{3} \frac{b^3}{c} \left(\frac{S_{12}}{S_{11}} + \frac{S_{66}}{S_{11}} - \frac{2S_{16}^2}{S_{11}^2} \right) - \frac{b}{c} \left(\frac{\ell^2}{4} - c^2 \right) \right.$$
$$\left. - \frac{4}{3} b^2 \frac{S_{16}}{S_{11}} + b^2 \left(\frac{S_{66}}{S_{16}} - \frac{2}{3} \frac{S_{16}}{S_{11}} \right) + \frac{\ell^2}{6} \frac{S_{11}}{S_{16}} \right] \tag{24}$$

yielding: /9

$$\frac{1}{E_{xx}^*} = \frac{\varepsilon_x^*}{\sigma_x^*} = S_{11} \left(1 - \eta_I\right) \tag{25}$$

with the subscript "I" referring to a Type I extensometer.

Whence, when ε_x^* and σ_x^* are replaced by the above expressions:

$$\eta_I = \frac{8S_{16}^2 + S_{16} \left[\frac{6}{bc} \left(\frac{\ell^2}{4} - c^2 \right) S_{11} + 2 \frac{b}{c} \left(S_{12} + S_{66} - 2\frac{S_{16}^2}{S_{11}} \right) \right]}{S_{11} \left(6S_{66} + \frac{\ell^2}{b^2} S_{11} \right) - 4 S_{16}^2} \tag{26}$$

If the extensometer is turned so that the feelers are at points A' and B', it then follows, in the same manner:

$$\eta'_I = \frac{8S_{16}^2 - S_{16}\left[\frac{6}{bc}\left(\frac{\ell^2}{4} - c^2\right) S_{11} + 2\,\frac{b}{c}\left(S_{12} + S_{66} - 2\frac{S_{16}^2}{S_{11}}\right)\right]}{S_{11}\left(6S_{66} + \frac{\ell^2}{b^2} S_{11}\right) - 4\,S_{16}^2} \tag{27}$$

Likewise, for a Type II extensometer:

$$\eta_{II} = \frac{8\,S_{16}^2}{S_{11}\left(6S_{66} + \frac{\ell^2}{b^2} S_{11}\right) - 4\,S_{16}^2} \tag{28}$$

The expression does not change if the extensometer is turned.

For the strain gauge:

$$\eta_{IV} = \frac{2\,S_{16}^2}{S_{11}\left(6S_{66} + \frac{\ell^2}{b^2} S_{11}\right) - 4\,S_{16}^2} \tag{29}$$

The Type III extensometer whose edges rest on the surface of the test piece should not be utilized for tests in oblique directions, since the edges thus rest along a line which will be warped, and the contact point of the feeler cannot be determined.

Therefore, for this type of test, the extensometer should be located along the edge of the test piece.

In summary, positing: /10

$$\begin{aligned}
\alpha &= 2\,S_{16}^2 \\
\beta &= S_{16}\left[\frac{6}{bc}\left(\frac{\ell^2}{4} - c^2\right) S_{11} + 2\,\frac{b}{c}\left(S_{12} + S_{66} - \frac{\alpha}{S_{11}}\right)\right] \\
\xi &= S_{11}\left(6\,S_{66} + \frac{\ell^2}{b^2} S_{11}\right) - 2\,\alpha
\end{aligned} \tag{30}$$

the correction coefficient expressions become:

$$\eta_I = \frac{4\alpha + \beta}{\xi} \qquad \eta_I' = \frac{4\alpha - \beta}{\xi}$$

$$\eta_{II} = \frac{4\alpha}{\xi} \qquad \eta_{IV} = \frac{\alpha}{\xi} \tag{31}$$

2.2.6 <u>Correction Coefficient for the Poisson Coefficient</u>

If the test piece is fitted qith a transverse gauge as shown in Figure 6, the expression of ε_y^* is given by relation (19) in which the v are replaced by their expression (15):

$$\varepsilon_y^* = -\frac{1}{6}\,\nu_{xy}\,C_0\,\frac{S_{11}}{S_{16}}\,[6S_{66}b^2 + S_{11}\,\ell^2 - 4\,\frac{S_{16}^2}{S_{11}}\,d^2] \tag{32}$$

With equation (23), C_0 can be expressed as a function of σ_x^*:

$$C_0 = \sigma_x^*\,\frac{6\,S_{16}}{[6S_{66}\,b^2 + S_{11}\,\ell^2 - 4\,\frac{S_{16}^2}{S_{11}}\,b^2]} \tag{33}$$

whence:

$$\varepsilon_y^* = -\,\nu_{xy}\,\sigma_x^*\,S_{11}\,\frac{6S_{66}\,b^2 + S_{11}\,\ell^2 - 4\,\frac{S_{16}^2}{S_{11}}\,d^2}{6S_{66}\,b^2 + S_{11}\,\ell^2 - 4\,\frac{S_{16}^2}{S_{11}}\,b^2} \tag{34}$$

Positing:

$$\psi = \frac{4\,S_{16}^2\,(\frac{d^2}{b^2} - 1)}{S_{11}\,(6\,S_{66} + S_{11}\,\frac{\ell^2}{b^2}) - 4\,S_{16}^2} \tag{35}$$

and utilizing relation (25), the expression of ε^*_y becomes: /11

$$\varepsilon^*_y = - \nu_{xy} \sigma^*_x S_{11} (1 - \psi)$$

$$\nu^*_{xy} = - \frac{\varepsilon^*_y}{\varepsilon^*_x} = \nu_{xy} \frac{(1 - \psi)}{(1 - \eta)} \qquad (36)$$

$$\nu_{xy} = \nu^*_{xy} (1 - \zeta) \qquad (37)$$

with

$$1 - \zeta = \frac{1 - \eta}{1 - \psi} \qquad (38)$$

The η to be taken into consideration is clearly that one corresponding to the type of extensometer utilized to measure ε^*_x.

3. Comparison of the Approximate Theory and the Finite Element Theory /12

3.1 General

In their publication "Deplacements, deformations et contraintes dans les materiaux elastiques anisotropes" [Displacements, Deformations and Strains in Anisotropic Elastic Materials] [3], R.M. Courtade et al. deal with the elaboration of the strain/deformation relation for an anisotropic elastic material, based on a procedure of calculations utilizing finite elements.

As illustrated in Figure 6, this method allows limit conditions which are slightly different from those set forth in Section 2.2.2.

Since this system is not symmetric with respect to the y-axis = $\frac{\ell}{2}$, in the case of the Type II extensometer, the results differ depending on whether the extensometer is placed to the left (at AB) or to the right (at A'B') of the test piece (Figure 6).

3.2 Comparison of Correction Coefficients Found by the Two Theories

These coefficients were calculated for a plate (1B in Table II) with the following characteristics:

Resin: rigid polyester
Reinforcement: unidirectional (23% glass by volume)

ℓ = 100 mm	E_{11} = 1914 kg/mm^2
b = 10 mm	E_{22} = 639 kg/mm^2
c = 25 mm	ν_{12} = 0.327
d = 5 mm	G_{12} = 257 kg/mm^2

As shown in Table I, the two theories yield correction coefficients which are relatively close, except in the case of the Type II extensometer. /13

These deviations principally result from limit conditions which are not the same in the two cases. The deviations for the $(1 - \zeta)$ coefficients are somewhat more significant.

This comparison allows us to conclude that the approximate theory is sufficiently correct to be utilized in a study of the influence of geometric parameters on test conditions.

4. Influence of Geometric Test Parameters on the Correction Coefficients /14

4.1 General

The influence of geometric parameters on the values of correction coefficients was studied for a material with the following characteristics: E_f = 7000 kg/mm^2; ν_f = 0.25; E_m = 395 kg/mm^2; ν_m = 0.35; ρ = 0.23. These characteristics are those of Plate 1B in Table II.

Moreover, the T_1 parameter will vary, being proportional to the quantity of fibers lying in direction 1. Thus, if $T_1 = 1$, the laminate is unidirectional; if $T_1 = 0.5$, the laminate is balanced and bidirectional; and, if $T_1 = 0$, the fibers all lie in direction 2. The symbols utilized for dimensions are defined in Figure 4 and Figure 5.

4.2 Influence of the Type of Extensometer and of T_1

Figure 7 illustrates for different values of T_1 the variation of different correction coefficients as functions of the angle θ formed by the principal direction 1 of the material with the x-axis of the test piece (Figure 3).

The geometric parameters selected for these calculations are those utilized for the tests, i.e.: $\ell = 100$ mm; $b = 10$ mm, with $c = 25$ mm for the Type I and Type II extensometers and $c = 5$ mm for the axial strain gauge.

It can be seen that the coefficients with respect to the Type I extensometer are the most significant. Then follow $(1 - \eta_{II})$ and /15
$(1 - \eta_{IV})$. With respect to the strain gauge, the latter is relatively weak. The correction factor $(1 - \psi)$ for the Poisson coefficient is also small. It can also be seen that when $T_1 = 1$, the greatest absolute value of these coefficients is obtained when angle $\theta \simeq 25°$.

4.3 Influence of the Length of the Test Piece

The curves shown in Figure 8 were calculated for $T_1 = 1, \theta \simeq 22.5°$ and $b = 10$ for different values of c, with ℓ being variable.

It should be noted that with respect to Type I extensometers, the $(1 - \eta_I)$ coefficients do not converge towards 1, contrary to supposition. This indicates that even if the test piece is quite long, a correction factor should be utilized with this type of extensometer.

The other factors converge rapidly towards 1.

4.4 Influence of the Length of the Extensometer Measurement Base

Figure 9 illustrates the influence of the relation c/ℓ on the value of the $(1 - \eta_I)$ and $(1 - \eta_I)$ coefficients. The other coefficients are not affected. The curves shown in Figure 9 were obtained for $\ell = 100$ mm, $b = 10$ mm, $T_1 = 1$ and $\theta = 22.5°$. In addition, Figure 9 shows the homologous curved obtained utilizing the finite element method.

4.5 Influence of the Length of the Strain Gauge Measuring ε_y

Figure 10 illustrates the influence of the relation d/b on the $(1 - \psi)$ factor with respect to the Poisson coefficient. This curve was also obtained for $T_1 = 1$, $\theta = 22.5°$, $b = 10$ mm and $\ell = 100$ mm, with d being variable.

5. Choice of a Type of Extensometer /16

Study of the influence of geometric parameters allows conclusions to be drawn concerning the type of extensometer and the dimensions of test pieces to be utilized in traction tests in oblique directions.

Working conditions must be those under which the correction coefficients are the smallest.

As noted above (Section 2.2.5), in order to measure ε_x, the Type II extensometer located on the surface of the test piece should not be utilized. The Type I extensometer utilized for tests should also be eschewed, since the corresponding correction coefficients do not converge towards 1 (see Figure 8). For measurement of ε_x, the two best types of extensometer are Type II and Type IV. Strain gauges are the most suitable to the extent that the operator is in complete control of their method of utilization on plastic materials.

To measure ε_y, it is preferable to utilize a strain gauge whose length is as nearly as possible equal to the width of the test piece. In any case, the value of the $(1 - \psi)$ coefficient is always very close to 1.

A transverse extensometer may also be utilized. In such tests, the ℓ/b ratio should be at least 20 in order to yield virtually negligible correction coefficients.

6. Test Results Compared to the Puck Theory /17

6.1 Test Method

The tests were carried out under the following conditions and with the equipment listed:

— test piece dimensions: see Figure 11

— test equipment: Tinius Olsen UEH Dynamic

— feeler displacement speed: 1.25 mm/minute

— extensometer: Tinius Olsen with 50 mm measurement base

— strain gauge: TML Type Pl 10; 10 mm

— load cell: Tinius Olsen 3 t.

6.2 Materials Tested

The materials tested were the same as those utilized in report [1]. The composition of these materials is given in Table II and their glass content is given in Table III.

6.3 Test Results

Test results are summarized in Table IV, where they are compared with the values obtained utilizing the Puck theory [1]. Table IV illustrates, respectively:

— the type of reinforcement:

U : unidirectional
U + M : unidirectional + mat
BE : balanced bidirectional
BE + M : balanced bidirectional + mat
B : bidirectional
B + M : bidirectional + mat

— the angle θ defined in Figure 3

— the theoretical values of E_{Puck} and ν_{Puck}

— the experimental values E^* and ν^* with the deviation in percent from theoretical values

— the corrected experimental values E_{exp} and ν_{exp} with the deviation in percent from the Puck theory

7. Conclusions /25

As shown in Table IV, the deviations obtained between the Puck theory and the experiments are satisfactory (less than 15%) in a majority of cases for measurement of the modulus of elasticity. Moreover, utilization of correction coefficients more often than not brought the measured value close to the theoretical value.

The deviations observed are slightly more important than they are for the principal directions, particularly for unbalanced laminates. This is due to the fact that only three tests were made for the latter directions, while five tests were made for the principal directions. Therefore, in the former case, the mean is less representative.

Some of the deviations obtained for Poisson coefficients are quite large, as was the case for the principal directions [1]. These large deviations are probably attributable to faulty attachment of the gauge to the test piece or to parasitic errors introduced into the measurement system. This has led us to conceive of a systematic study of the use of gauges on plastic materials. This study will be carried out in the next few months. It is in fact important to answer the question raised by an author: "Do we measure strain when we measure strain?" Current work indicates that sometimes this question must be answered in the negative, and it is absolutely essential to resolve this problem if we are to obtain a better understanding of the behavior of reinforced plastics.

8. Acknowledgements

/26

We are deeply thankful to Madame R.M. Courtade, Ph.D., engineer at the Institut National des Sciences Appliques [National Applied Sciences Institute] (INSA) of Lyon, who, with the aid of her finite element program, resolved for us the problem of the deformation of anisotropic test pieces.

Our thanks are also due to Mr. Manera, engineer at the Centre Europeen de Recherche et Essais [European Research and Testing Center] (CERE) of the Fiberglass Division of Saint-Gobain Industries for his much-appreciated assistance and always constructive criticism.

Lastly, we thank the Belgian industrial members of the Fabriplast Group of Fabrimetal for the assistance and encouragement they always gave our work, and particularly Mr. Orlians and Mr. Vivile, the president and secretary, respectively, of Fabriplast.

REFERENCES

/27

1. Lacrosse, B., Massonnet, C., Viatour, G. and Vidouse, F., "Theoretical and Experimental Study of the Technical Constants of Laminates" (CRIF PL 3, June 1972)

2. Pagano, N.J. and Halpin, J.C., "Influence of End Constraint in the Testing of Anisotropic Bodies", J.Comp.Mat. 2, 18 (1968)

3. Courtade, R.M., Lemaire, M. and Cubaud, J.C., "Deplacements, deformations et contraintes dans les materiaux elastiques anisotropes" [Displacements, Deformations and Strains in Anisotropic Elastic Materials], Verre Textile/Plastiques Renforces [Fiberglass/Reinforced Plastics], June 1973

4. Ashton, J.E. and Whitney, J.M., Theory of Laminated Plates, Technomic Publishing Co. [n.d.]

Table I. Comparison of the correction coefficients yielded by the two theories

0	22,5°			45°			67,5°		
Coefficient	Approx. theory	Finite elements	Deviation %	Approx. theory	Finite elements	Deviation %	Approx. theory	Finite elements	Deviation %
$1 - \eta_I$	1,2844	1,3217	2,80	1,1445	1,1521	0,92	1,0007	1,0076	0,68
$1 - \eta'_I$	0,6172	0,6448	4,30	0,8356	0,8430	0,87	0,9993	0,9941	- 0,52
$1 - \eta_{II}$	0,9508	0,8435	- 12,70	0,9900	0,9249	- 7,00	1,0000	0,9935	- 0,65
$1 - \eta'_{II}$	0,9508	1,1231	15,30	0,9900	1,0699	7,50	1,0000	1,0082	0,81
$1 - \eta_{IV}$	0,9877	0,9951	0,70	0,9975	0,9986	0,11	1,0000	1,0001	0,01
$1 - \zeta_I$	1,2844	1,4558	11,80	1,1399	1,2280	7,25	0,9827	1,0521	6,60
$1 - \zeta'_I$	0,6172	0,7116	13,30	0,8323	0,9007	7,59	0,9813	1,0374	5,40
$1 - \zeta_{II}$	0,9508	0,9300	- 2,15	0,9860	0,9870	0,10	0,9820	1,0374	5,30
$1 - \zeta'_{II}$	0,9508	1,2372	23,10	0,9860	1,1441	13,82	0,9820	1,0521	6,70
$1 - \zeta_{IV}$	0,9877	1,0987	10,10	0,9935	1,0672	6,91	0,9820	1,0423	5,80

Table II. Plate composition

Resins : P = flexible polyester (Palatal P51) ($E = 274$ kg/mm^2 ; $\nu = 0{,}366$)
B = rigid polyester (Stratyl B) ($E = 395$ kg/mm^2 ; $\nu = 0{,}350$)
E = rigid epoxy (Ciba LY556) ($E = 342$ kg/mm^2 ; $\nu = 0{,}294$)

Plate No.	Type of reinforcement	Brand Name	Gr/m^2	Number of layers	Method of manufacture
1 P	Satin	Porcher 716bis	200	17	Press
5 P	Satin	Porcher 716bis	200	6	"
	Mat	Gevetex M 512	450	3	"
9 P	Satin	Tissaverre 158	308	11	"
14 P	Taffetas	Tissaverre 249	200	16	"
17 P	Satin	Tissaverre 158	308	4	"
	Mat	Gevetex M 512	450	3	"
18 P	Taffetas	Tissaverre 249	200	6	"
	Mat	Gevetex M 512	450	3	"
19 P	Mat	Gevetex M 512	450	4	"
23 P	Preformed				"
25 P	Spray up				Spray up
1 B	Uni-directional	Verester 29	400	5	Contact
5 B	Catching rov.	Cotton 5283	420	4	"
9 B	Taffetas	Verester 39	500	4	"
13 B	Serge	Verester 131	470	4	"
17 B	Mats	M1.100.P23	450	3	"
21 B	Mats	M4.400.P3	450	3	"
25 B	Unidir.	Verester 29	400	2	"
	Mats	M1.100.P23	450	2	"
29 B	Taffetas	Verester 39	500	2	"
	Mat	M1.100.P23	450	2	"
30 B	Serge	Verester 131	470	2	"
	Mat	M1.100.P23	450	2	"
31 B	Spray up				Spray up
34 B	Preformed				Presse
36 B	Mat	Gevetex M512	450	4	"
38 B	Satin	Porcher 716bis	200	17	"
40 B	Taffetas	Tissaverre 249	200	16	"
44 B	Satin	Tissaverre 158	308	11	"
48 B	Satin	Porcher 716bis	200	6	"
	Mats	Gevetex M 512	450	3	"
52 B	Taffetas	Tissaverre 249	200	6	"
	Mat	Gevetex M 512	450	3	"
53 B	Satin	Tissaverre 158	308	4	"
	Mat	Gevetex M 512	450	3	"
1 E	Satin	Tissaverre 158	308	11	Presse
3 E	Satin	Porcher 716bis	200	17	"
5 E	Taffetas	Tissaverre 249	200	16	"
7 E	Unidir.	Verester 764	610	3	Contact
9 E	Taffetas	Verester 39	500	4	"

Table III. Glass contents

T = Glass content by weight

ϕ = Glass content by volume

m = Glass content per square meter (m^2)

Plate No.	T (%)	ϕ	m gr/m^2
1 P	61.46	0.426	3274
5 P	51.29	0.315	2361
9 P	61.80	0.440	3270
13 P	64.06	0.455	3432
17 P	53.40	0.337	2545
18 P	56.42	0.362	2708
19 P	41.92	0.249	1854
23 P	37.32	0.219	1637
25 P	26.69	0.147	1638
1 B	38.88	0.23	2106
5 B	33.84	0.19	1642
9 B	41.92	0.24	1999
13 B	42.67	0.25	2235
17 B	26.86	0.14	1253
21 B	24.73	0.13	1147
25 B	32.87	0.19	1517
29 B	38.52	0.23	1748
30 B	35.87	0.20	1828
31 B	31.11	0.18	1221
34 B	37.09	0.21	1598
36 B	39.82	0.22	1727
38 B	59.44	0.40	3057
40 B	63.95	0.45	3404
44 B	61.59	0.43	3241
48 B	51.97	0.32	2438
52 B	53.70	0.33	2548
53 B	52.48	0.32	2475
1 E	61.48	0.41	3241
3 E	60.98	0.41	3287
5 E	62.40	0.42	3380
7 E	42.49	0.25	1883
9 E	45.39	0.26	2058

Table IV. Experimental results compared to the Puck theory

Type of reinforcement	Plate No.	ε (%)	E_{Puck} kg/mm²	E^* kg/mm²	Deviation in % $\frac{E_{Puck} - E^*}{E^*} \times 100$	E_{exp} kg/mm²	Deviation in % $\frac{E_{Puck} - E_{exp}}{E_{exp}} \times 100$	ν_{Puck}	ν^*	Deviation in % $\frac{\nu_{Puck} - \nu}{\nu^*} \times 100$	ν_{exp}	Deviation in % $\frac{\nu_{Puck} - \nu_{exp}}{\nu_{exp}} \times 100$
U	1 B	0,0	639	730	- 12,5	730	- 12,5	0,109	0,106	3,0	0,106	3,0
		22,5	627	663	- 5,4	663	- 5,4	0,222	0,225	- 1,4	0,225	- 1,4
		45,0	709	682	4,0	609	16,5	0,381	0,461	- 17,4	0,404	- 5,7
		67,5	1165	1226	- 4,9	1441	- 19,1	0,412	0,355	16,1	0,417.	- 1,2
		90,0	1914	1669	14,7	1669	14,7	0,327	0,297	10,1	0,297	10,1
	7 E	0,0	2006	2079	- 3,5	2079	- 3,5	0,283	0,310	- 8,7	0,310	- 8,7
		22,5	1133	1112	1,8	1458	- 22,3	0,379	0,385	- 1,6	0,492	- 23,0
		45,0	650	647	0,5	753	- 13,7	0,343	0,264	30,0	0,307	11,7
		67,5	554	665	- 16,8	653	- 15,2	0,185	0,240	- 22,9	0,236	- 21,6
		90,0	554	757	- 26,8	757	- 26,8	0,078	0,094	- 16,8	0,094	- 16,8
U + M	25 B	0,0	792	692	14,4	692	14,4	0,198	0,233	- 15,0	0,233	- 15,0
		22,5	776	776	- 1,1	779	- 0,4	0,268	0,271	- 1,0	0,269	- 0,3
		45,0	823	823	31,7	674	22,1	0,363	0,275	32,1	0,297	22,3
		67,5	1053	1053	- 4,0	1252	- 15,9	0,364	0,280	30,0	0,318	14,5
		90,0	1276	1276	19,6	1067	19,6	0,319	0,319	0,0	0,319	0,0
BE	5 B	0,0	1132	1231	- 8,0	1231	- 8,0	0,175	0,191	- 8,2	0,191	- 8,2
		22,5	869	896	- 3,0	921	- 5,7	0,367	0,338	8,6	0,344	6,7
		45,0	705	806	- 12,5	806	- 12,5	0,487	0,456	6,7	0,456	6,7
	9 B	0,0	1328	1313	1,1	1313	1,1	0,161	0,162	- 0,4	0,162	- 0,4
		22,5	989	1109	- 10,8	861	14,8	0,375	0,358	4,9	0,276	35,9
		45,0	788	740	6,4	740	6,4	0,503	0,407	23,5	0,407	23,5
	40 B	00,0	2227	2529	- 12,0	2529	- 12,0	0,145	0,175	- 17,2	0,175	- 17,2
		22,5	1604	2040	- 21,4	1536	4,4	0,384	0,382	0,4	0,286	34,3
		45,0	1254	1558	- 19,5	1558	- 19,5	0,519	0,409	26,8	0,409	26,8

Table IV. Continued

Type of reinforcement	Plate No.	θ (°)	E_{puck} kg/mm²	E^* kg/mm²	Deviation in % $\frac{E_{Puck} - E^*}{E^*} \times 100$	E_{exp} kg/mm²	Deviation in % $\frac{E_{Puck} - E_{exp}}{E_{exp}} \times 100$	ν_{Puck}	ν^*	Deviation in % $\frac{\nu_{Puck} - \nu^*}{\nu^*} \times 100$	ν_{exp}	Deviation in % $\frac{\nu_{Puck} - \nu_{exp}}{\nu_{exp}} \times 100$
BE (cont.)	44 B	0,0	2133	2382	- 10,4	2382	- 10,4	0,145	0,155	- 6,7	0,155	- 6,7
		22,5	1534	1811	- 15,3	1362	12,6	0,385	0,399	- 3,6	0,298	29,2
		45,0	1197	1377	- 13,1	1377	- 13,1	0,520	0,450	15,6	0,450	15,6
	9 P	0,0	2000	2042	- 2,1	2042	- 2,1	0,116	0,117	- 0,8	0,117	- 0,8
		22,5	1240	997	24,4	1402	- 11,5	0,452	0,512	- 11,7	0,356	27,0
		45,0	899	747	20,3	747	20,3	0,603	0,600	0,5	0,600	0,5
	13 P	0,0	2066	2202	- 6,2	2202	- 6,2	0,116	0,136	- 14,4	0,136	- 14,4
		22,5	1284	1603	19,9	1084	18,4	0,451	0,363	24,2	0,481	- 6,2
		45,0	931	1283	- 27,4	1283	- 27,4	0,602	0,471	27,8	0,471	27,8
	1 E	0,0	1946	2149	- 9,4	2149	- 9,4	0,113	0,116	- 2,3	0,116	- 2,3
		22,5	1356	1456	- 6,9	1404	- 3,4	0,382	0,377	1,2	0,360	6,1
		45,0	1041	1191	- 12,6	1191	- 12,6	0,526	0,546	- 3,7	0,546	- 3,7
	5 E	0,0	1990	2211	- 10,0	2211	- 10,0	0,114	0,154	- 26,3	0,154	- 26,3
		22,5	1387	1788	- 22,4	1344	3,2	0,382	0,406	- 6,0	0,314	21,7
		45,0	1065	1332	- 20,1	1332	- 20,1	0,526	0,518	1,5	0,518	1,5
	9 E	0,0	1329	1349	- 1,5	1349	- 1,5	0,121	0,142	- 14,7	0,142	- 14,7
		22,5	955	1021	- 6,5	947	0,8	0,369	0,367	0,3	0,339	8,8
		45,0	745	954	- 21,9	954	- 21,9	0,507	0,560	- 9,4	0,560	- 9,4
BE + M	29 B	0,0	1189	1160	2,5	1160	2,5	0,228	0,155	47,3	0,155	47,3
		22,5	1036	1014	2,2	968	7,0	0,328	0,351	- 6,6	0,336	- 2,4
		45,0	917	793	15,7	793	15,7	0,404	0,390	3,7	0,390	3,7
	52 B	0,0	1537	1640	- 6,3	1640	- 6,3	0,227	0,273	- 16,7	0,273	- 16,7
		22,5	1345	1601	- 16,0	1432	- 6,1	0,324	0,366	- 11,7	0,327	- 0,9
		45,0	1196	1088	9,9	1088	9,9	0,399	0,324	23,0	0,324	23,0
	53 B	0,0	1502	1473	2,0	1473	2,0	0,226	0,222	1,9	0,222	1,9
		22,5	1312	1553	- 15,5	1385	- 5,3	0,324	0,415	- 21,8	0,370	- 12,4
		45,0	1164	1128	3,2	1128	3,2	0,400	0,350	14,4	0,350	14,4

Table IV. Continued

Type of reinforcement	Plate No.	θ (°)	E_{Puck} kg/mm²	E^* kg/mm²	Deviation in % $\frac{E_{Puck} - E^*}{E^*} \times 100$	E_{exp} kg/mm²	Deviation in % $\frac{E_{Puck} - E_{exp}}{E_{exp}} \times 100$	ν_{Puck}	ν^*	Deviation in % $\frac{\nu_{Puck} - \nu^*}{\nu^*} \times 100$	ν_{exp}	Deviation in % $\frac{\nu_{Puck} - \nu_{exp}}{\nu_{exp}} \times 100$
EE + M (cont.)	17 P	0,0	1399	1362	2,7	1362	2,7	0,214	0,214	0,1	0,214	0,1
		22,5	1164	1164	0,1	1198	- 2,8	0,346	0,318	8,6	0,328	5,5
		45,0	997	1057	- 5,7	1057	- 5,7	0,440	0,340	29,4	0,340	29,4
	18 P	0,0	1485	1403	5,9	1403	5,9	0,215	0,205	4,9	0,205	4,9
		22,5	1240	1028	20,7	1190	- 4,2	0,345	0,274	25,8	0,316	9,2
		45,0	1064	1091	- 2,5	1091	- 2,5	0,438	0,344	27,2	0,344	27,2
B	13 B	0,0	1603	1543	3,9	1543	3,9	0,193	0,160	20,4	0,160	20,4
		22,5	1098	1111	- 1,2	1366	- 19,6	0,405	0,327	23,9	0,398	1,8
		45,0	799	674	18,5	703	13,6	0,493	0,431	14,4	0,450	9,6
		67,5	913	1238	- 26,3	1086	- 16,0	0,337	0,431	- 21,9	0,361	- 6,6
		90,0	1130	1236	- 8,6	1236	- 8,6	0,136	0,148	- 8,3	0,148	- 8,3
	38 B	0,0	2526	2740	- 7,8	2740	- 7,8	0,197	0,200	- 1,4	0,200	- 1,4
		22,5	1604	1760	- 8,9	2220	- 27,8	0,423	0,358	18,1	0,444	- 4,7
		45,0	1098	1223	- 10,2	1139	- 3,6	0,493	0,373	32,2	0,357	38,1
		67,5	1209	1517	- 20,3	1304	- 7,3	0,319	0,359	- 11,3	0,307	3,9
		90,0	1462	1489	- 1,8	1489	- 1,8	0,114	0,102	11,9	0,102	11,9
	1 P	0,0	2550	2835	- 10,1	2835	- 10,1	0,170	0,208	- 18,4	0,208	- 18,4
		22,5	1340	1328	0,9	1753	- 23,6	0,492	0,344	43,1	0,443	11,1
		45,0	850	1068	- 20,4	1000	- 15,0	0,568	0,430	32,2	0,401	41,6
		67,5	996	1491	- 33,2	1182	- 15,7	0,366	0,404	- 9,4	0,319	14,7
		90,0	1323	1346	- 1,7	1346	- 1,7	0,088	0,087	1,2	0,087	1,2
	3 E	0,0	2517	2792	- 9,9	2792	- 9,9	0,161	0,209	- 23,1	0,209	- 23,1
		22,5	1525	1553	- 1,8	1985	- 23,2	0,417	0,411	1,5	0,516	- 19,2
		45,0	1017	1222	- 16,7	1132	- 10,1	0,492	0,526	- 6,5	0,487	1,0
		67,5	1123	1221	- 8,0	1042	7,8	0,307	0,334	- 8,0	0,284	8,1
		90,0	1371	1401	- 2,1	1401	- 2,1	0,088	0,085	3,0	0,085	3,0

Table IV. Continued

Type of reinforcement	Plate No.	θ (°)	E_{Puck} kg/mm²	E^* kg/mm²	Deviation in % $\frac{E_{Puck} - E^*}{E^*} \times 100$	E_{exp} kg/mm²	Deviation in % $\frac{E_{Puck} - E_{exp}}{E_{exp}} \times 100$	ν_{Puck}	ν^*	Deviation in % $\frac{\nu_{Puck} - \nu^*}{\nu^*} \times 100$	ν_{exp}	Deviation in % $\frac{\nu_{Puck} - \nu_{exp}}{\nu_{exp}} \times 100$
B + M	30 B	0,0	984	996	- 1,2	996	- 1,2	0,218	0,140	55,4	0,140	55,4
		22,5	898	806	11,5	859	4,6	0,307	0,293	4,9	0,312	- 1,6
		45,0	850	813	4,6	816	4,2	0,394	0,447	- 11,9	0,449	- 12,2
		67,5	1003	988	1,5	1101	- 8,9	0,343	0,350	- 2,0	0,389	- 11,8
		90,0	1174	1155	1,6	1155	1,6	0,260	0,171	51,8	0,171	51,8
	48 B	0,0	1693	1928	- 12,2	1928	- 12,2	0,262	0,323	- 18,8	0,323	- 18,8
		22,5	1414	1459	- 3,1	1507	- 6,2	0,347	0,372	- 6,7	0,380	- 8,7
		45,0	1162	995	16,8	1037	12,0	0,391	0,322	21,3	0,336	16,4
		67,5	1201	1149	4,5	1164	3,2	0,295	0,296	- 0,4	0,299	- 1,3
		90,0	1302	1145	13,7	1145	13,7	0,202	0,190	6,1	0,190	6,1
	5 P	0,0	1524	1617	- 5,7	1617	- 5,7	0,258	0,250	3,3	0,250	3,3
		22,5	1200	1095	9,6	1275	- 5,9	0,373	0,305	22,2	0,353	5,7
		45,0	942	944	- 0,2	966	- 2,5	0,426	0,322	32,2	0,331	28,7
		67,5	992	844	17,6	1071	- 7,3	0,308	0,225	37,1	0,286	7,7
		90,0	1108	936	18,4	936	18,4	0,188	0,145	29,5	0,145	29,5

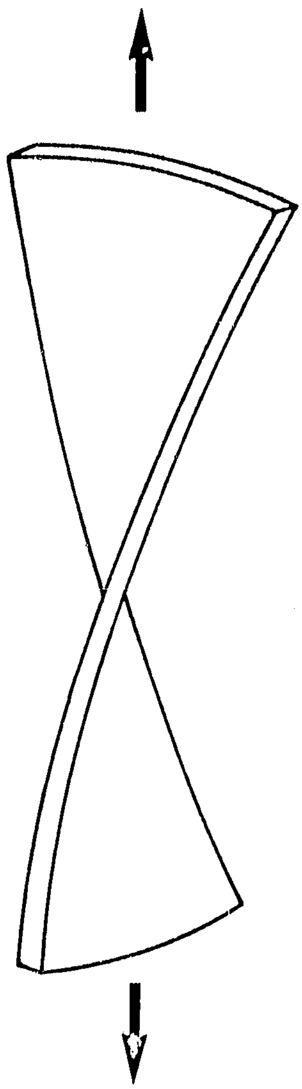

Figure 1. Deformation of an Anisotropic Test Piece

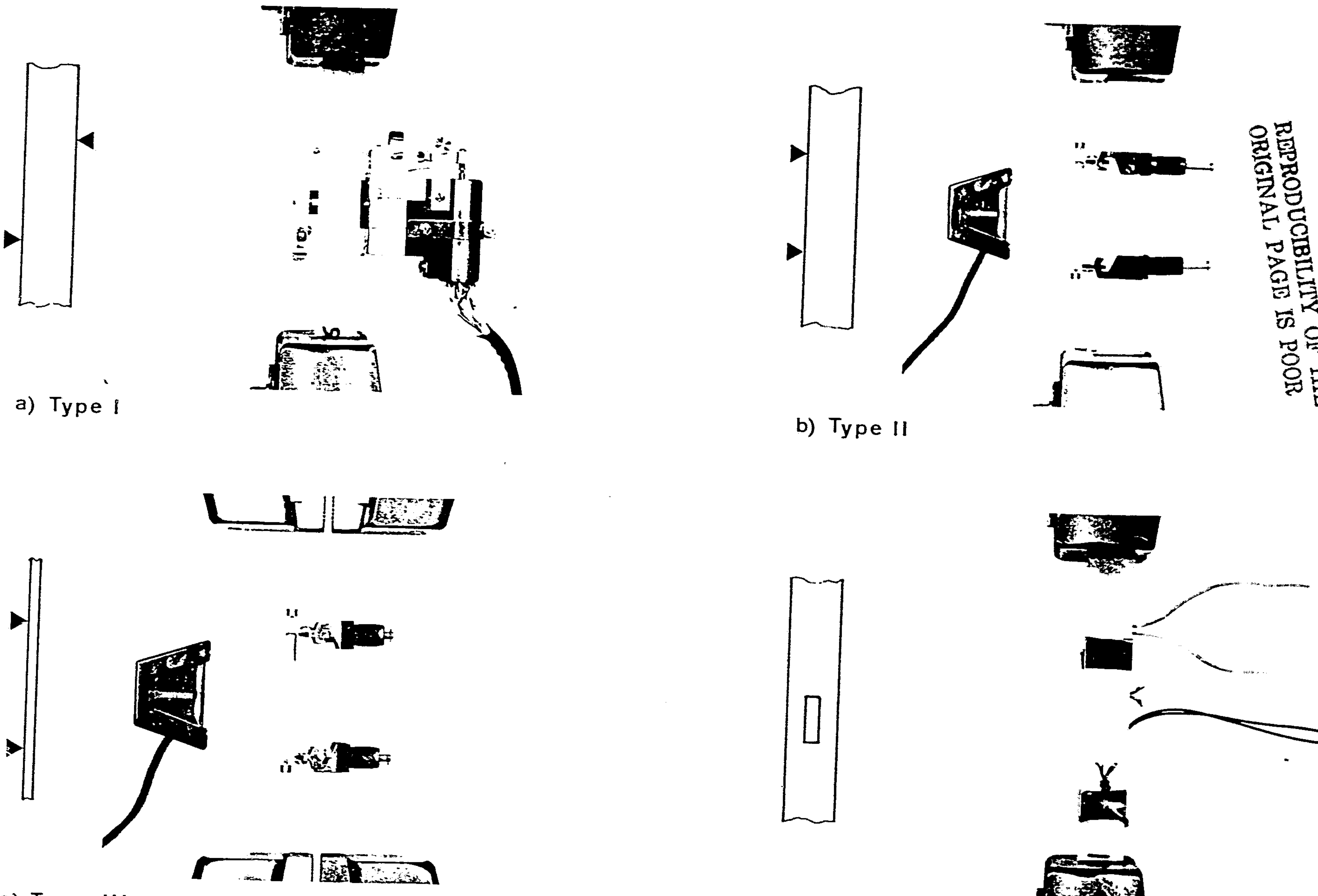

a) Type I

b) Type II

c) Type III

d) Type IV

Figure 2. Types of Extensometers

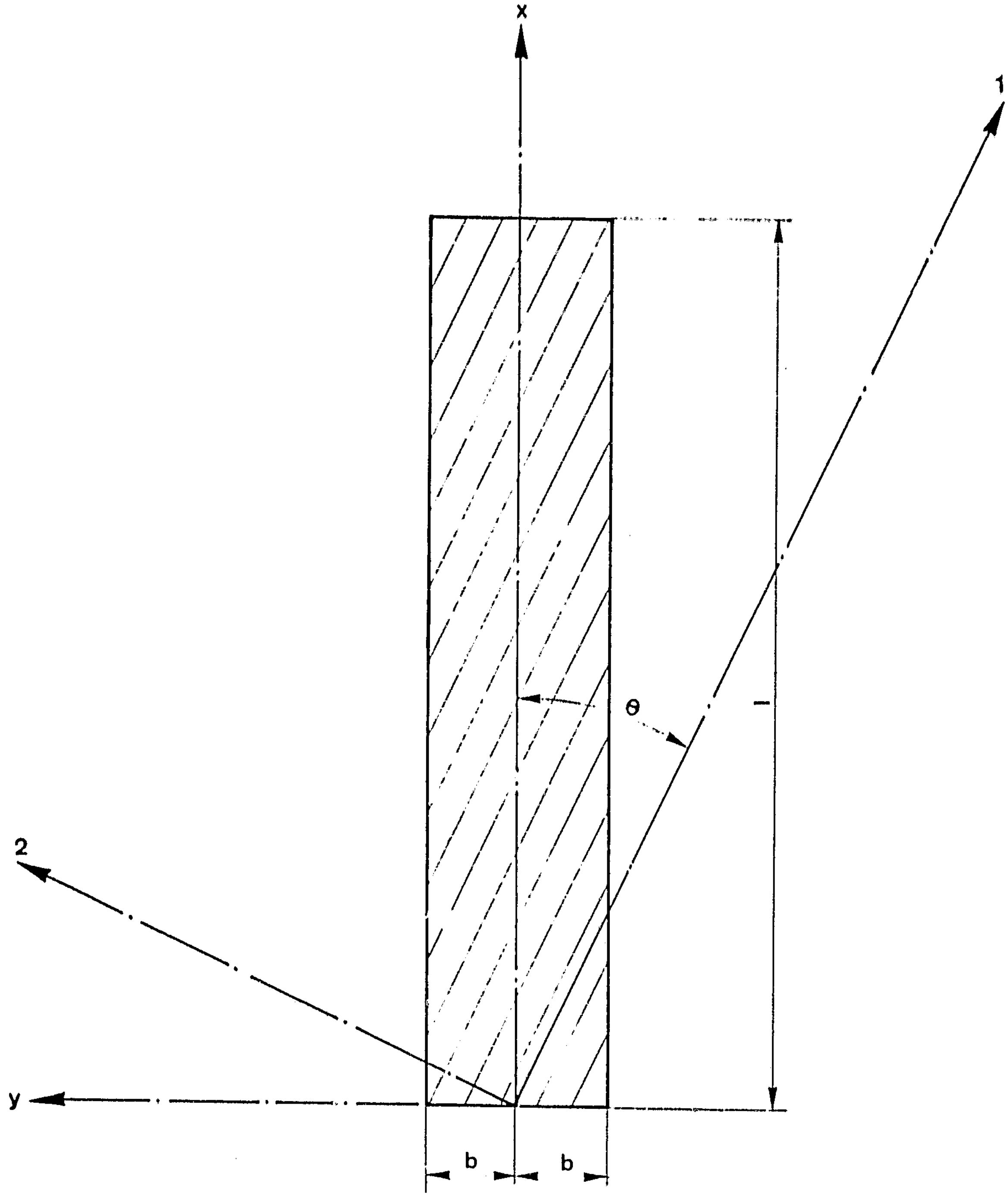

Figure 3. Orientation of Reference Axes

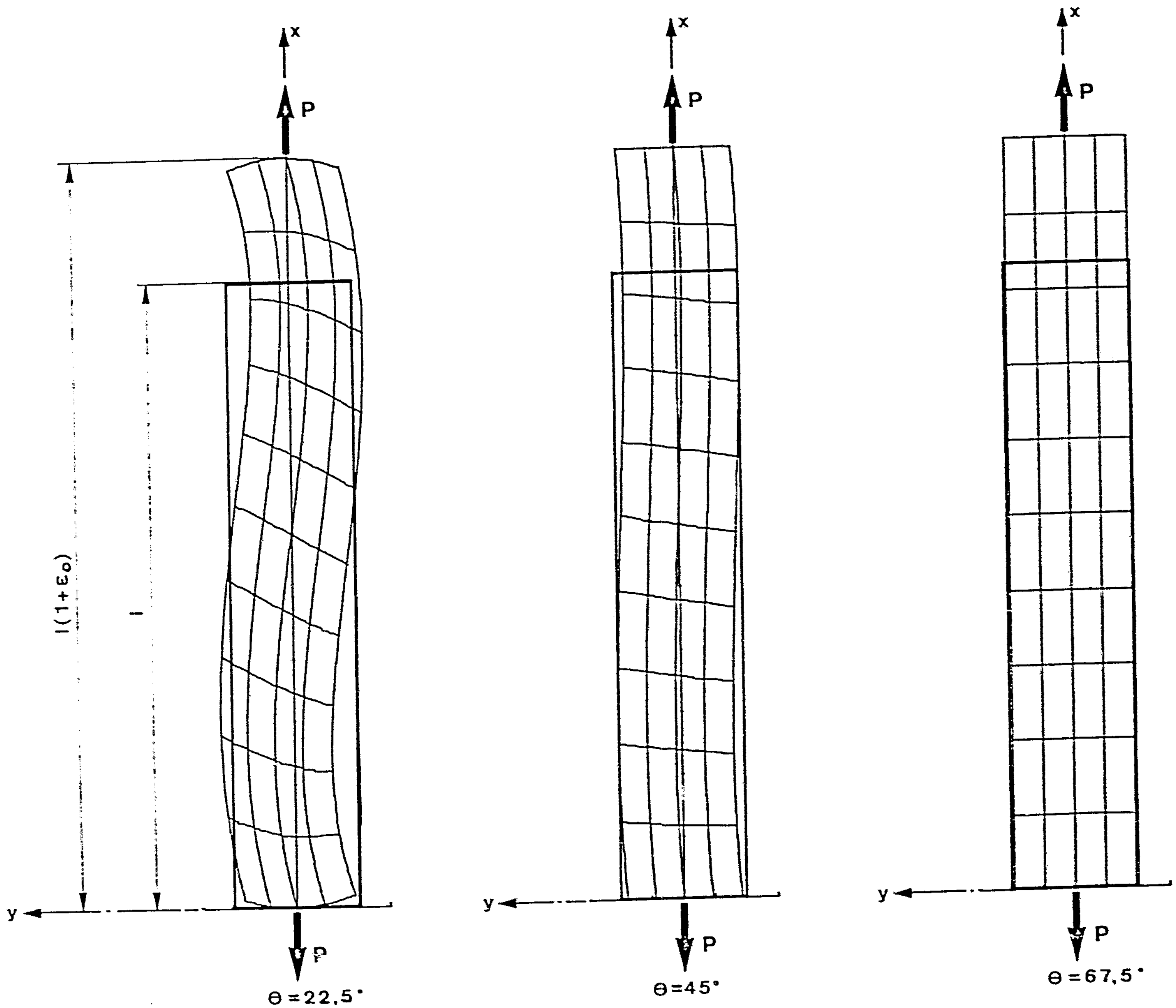

Figure 4. Deformation of a Unidirectional Test Piece under Simple Traction for Various Reinforcement Orientations θ

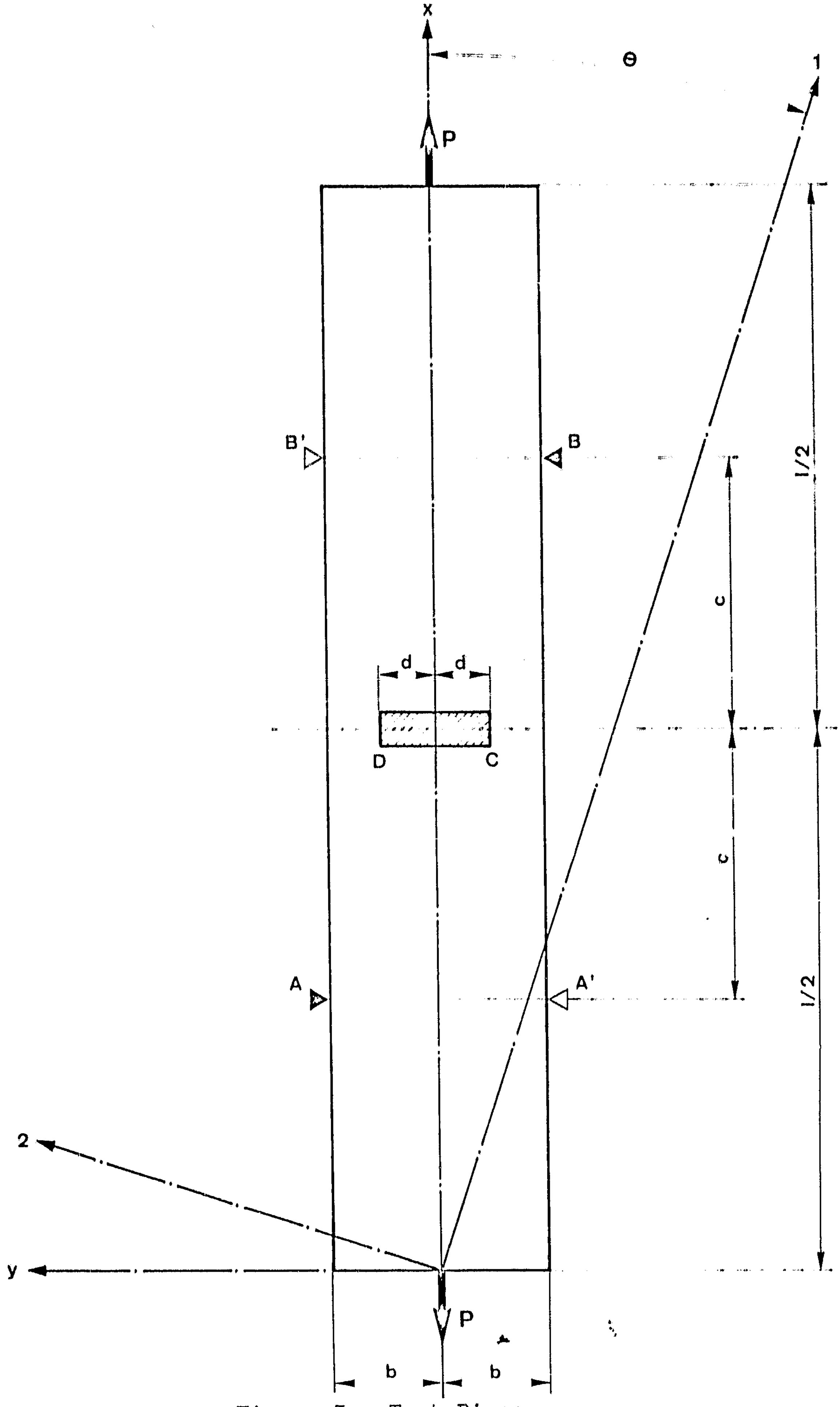

Figure 5. Test Piece

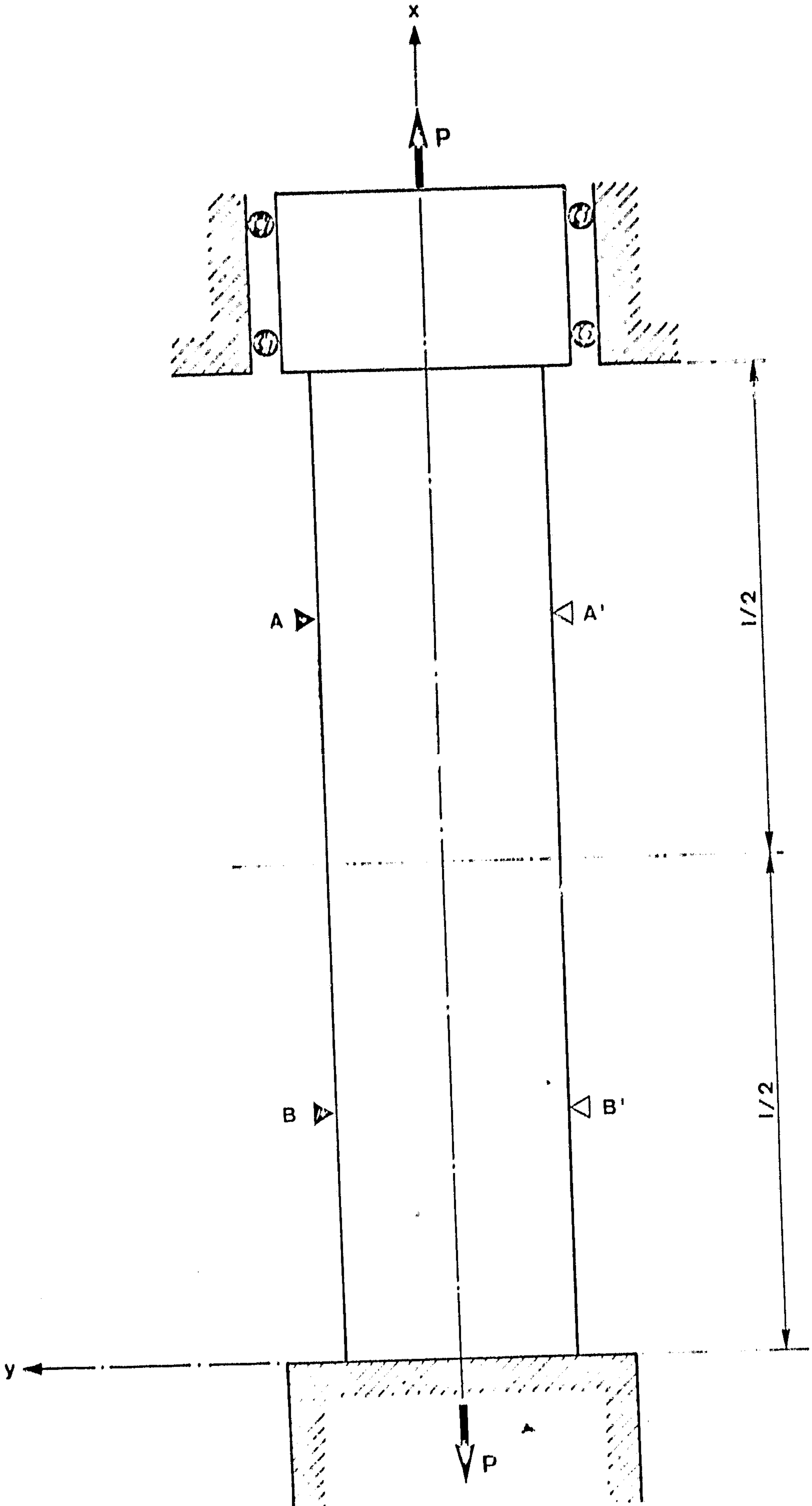

Figure 6. Limit Conditions Utilized by the Finite Element Theory

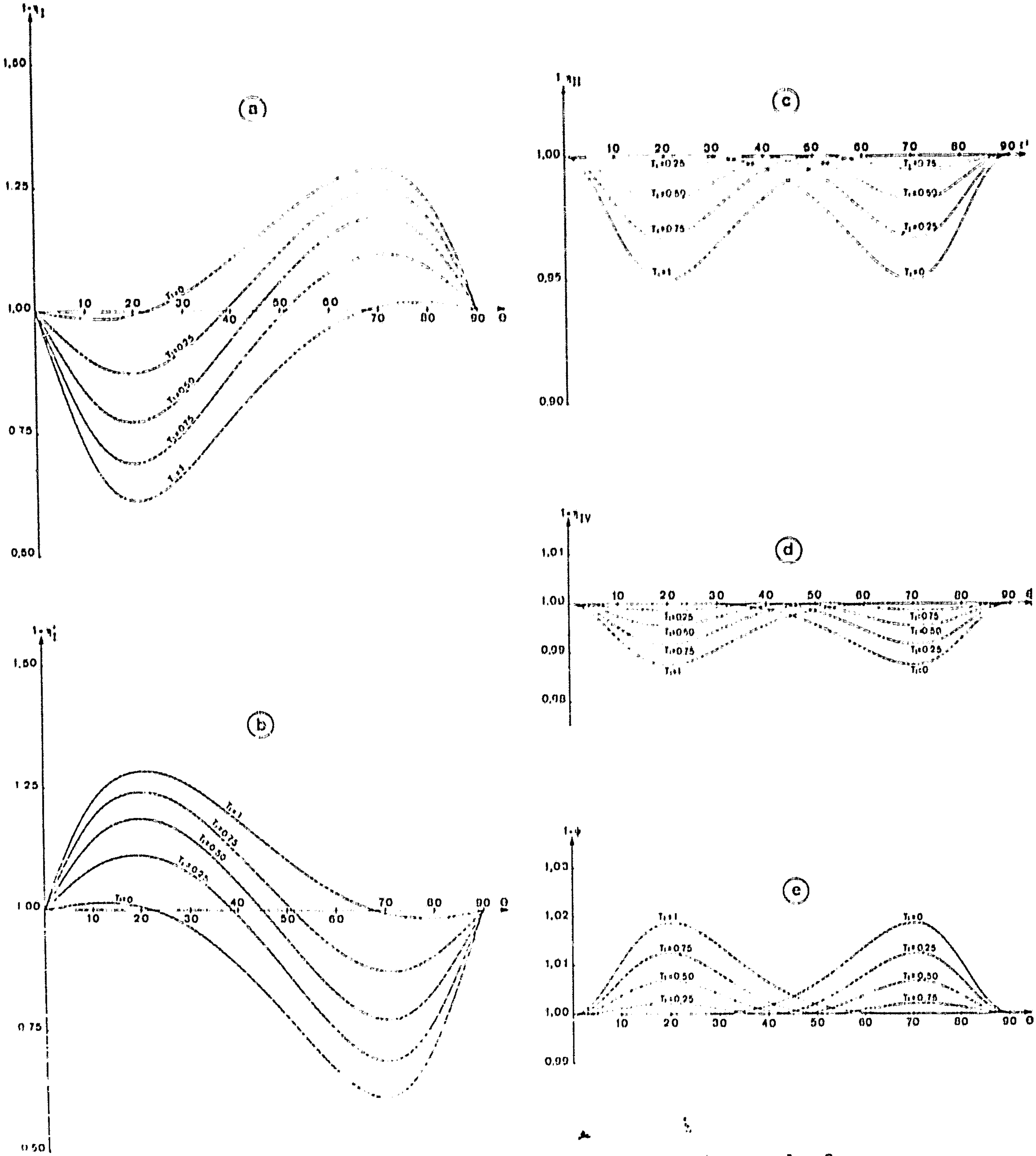

Figure 7. Influence of the Type of Extensometer and of T_1 on Correction Coefficients

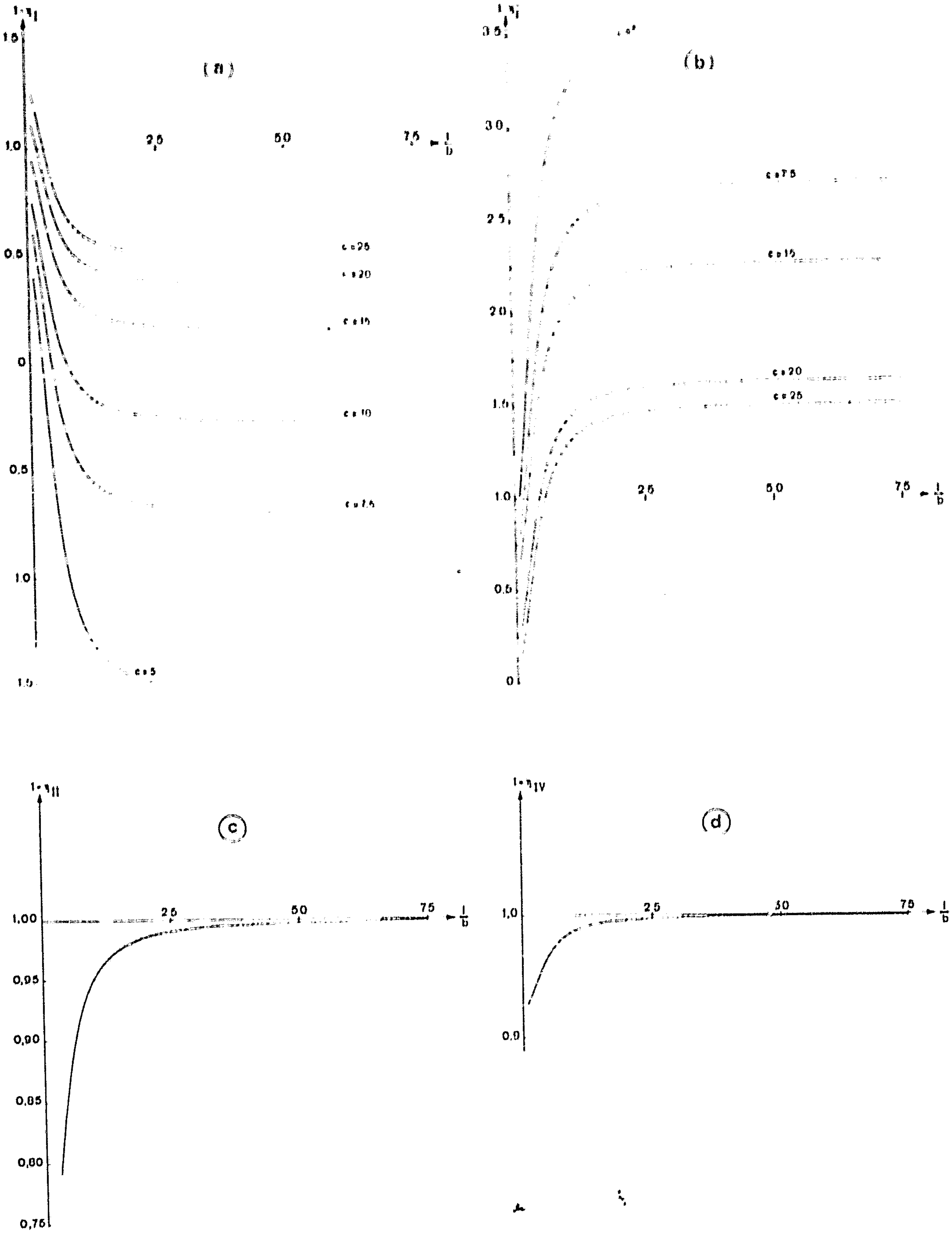

Figure 8. Influence of the Length of the Test Piece

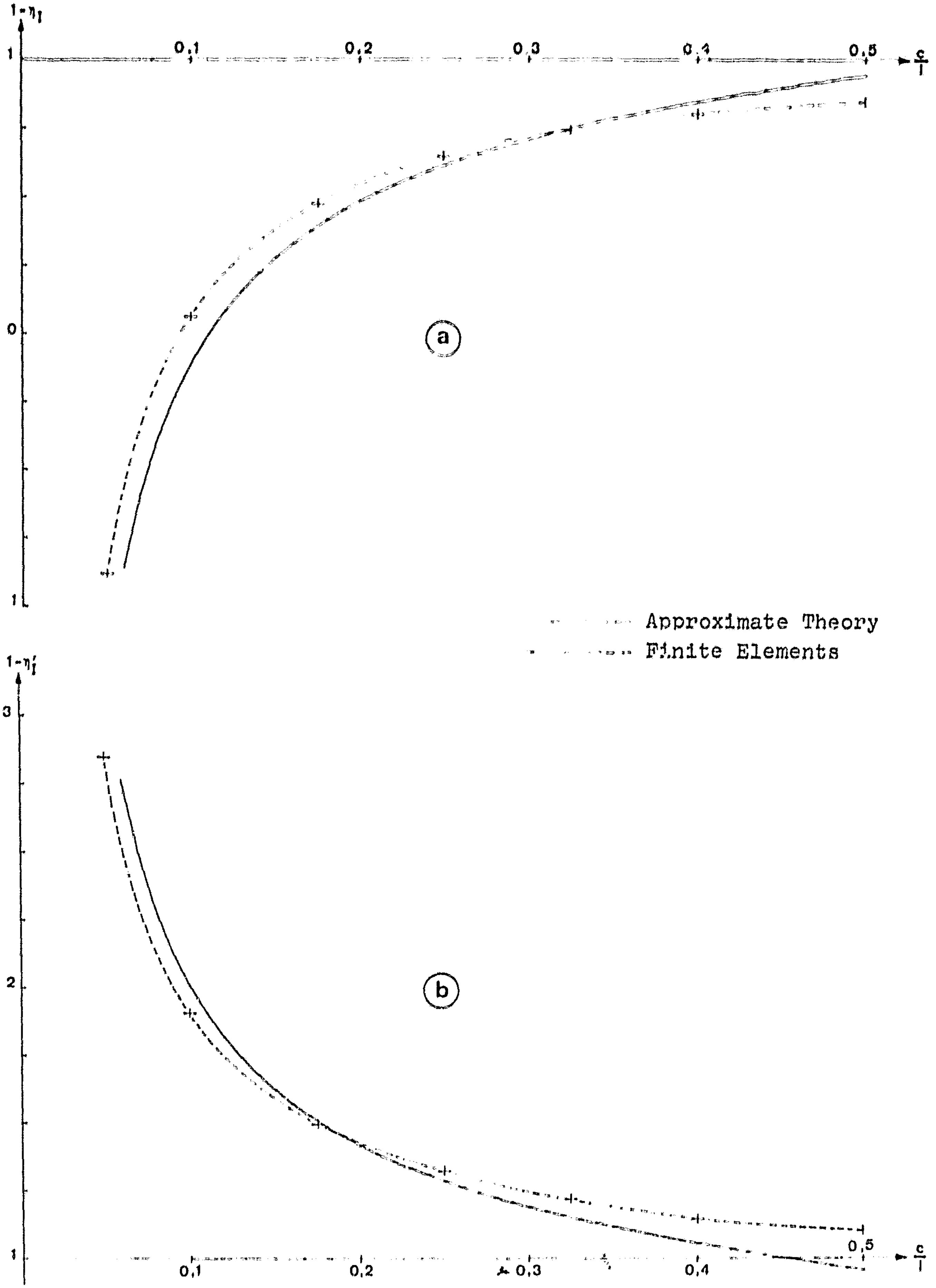

Figure 9. Influence of the Length of the Extensometer Measurement Base

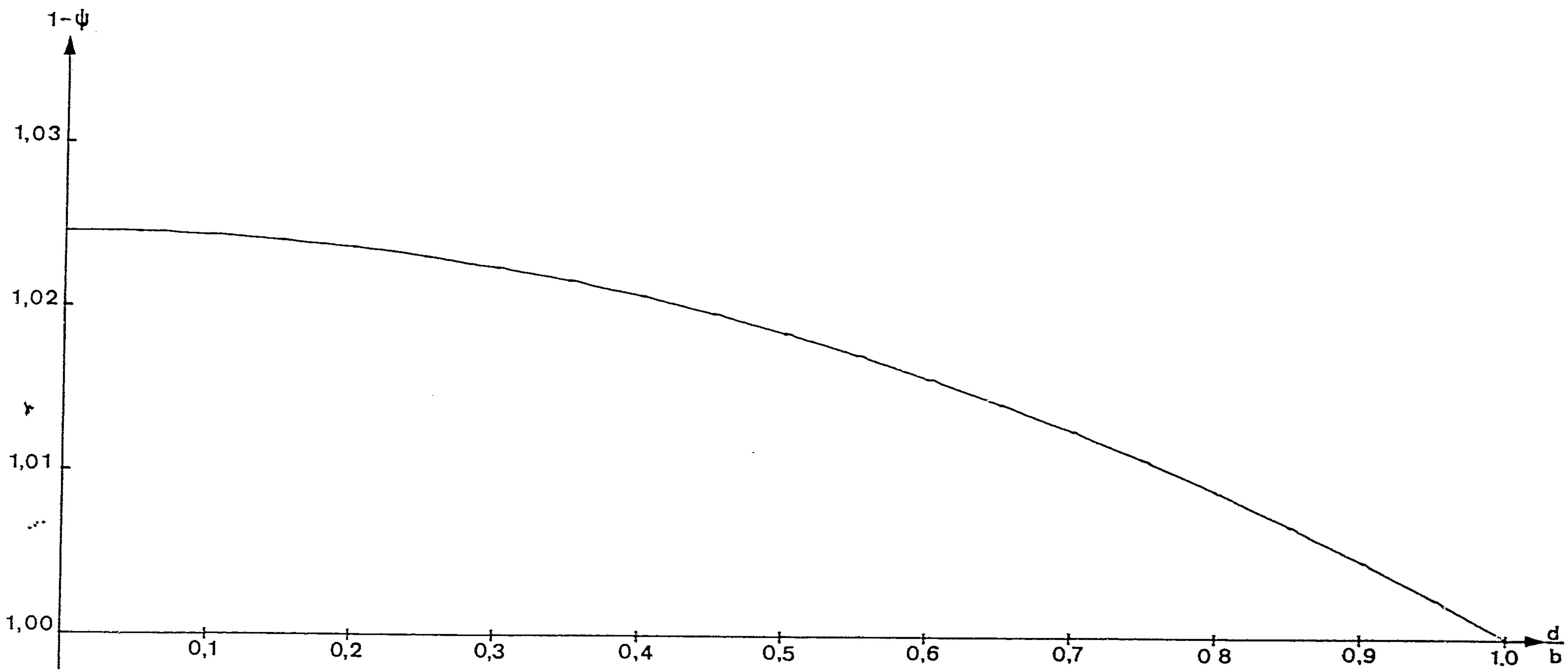

Figure 10. Influence of the Length of the Guage Measuring ε_y

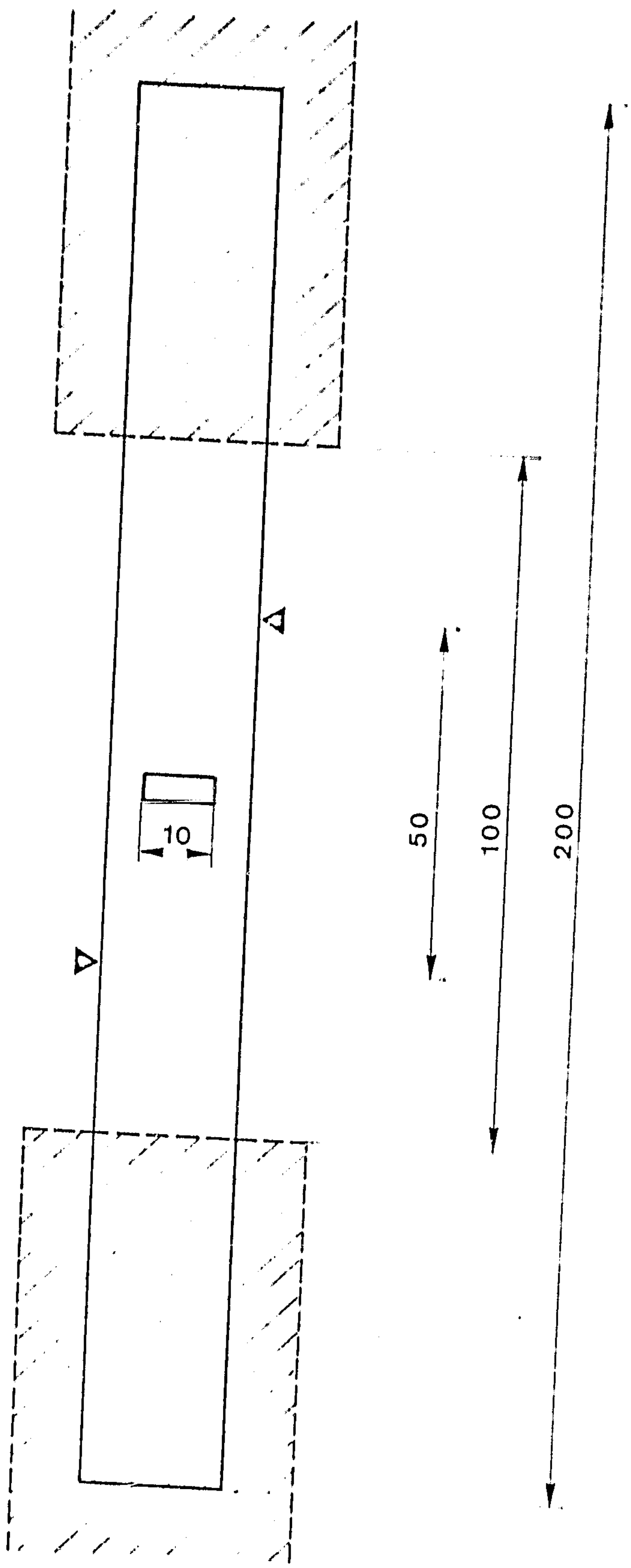

Figure 11. Test Piece Dimensions (in mm)